

Study on the effect of the plasma current overshoot in KSTAR

M.S. Park¹, Y.-S. Na^{1*}, J. Seo¹, B. Kim¹, C.Y. Lee¹, Y.H. Lee² and S.K. Kim³

¹ Department of Nuclear Engineering, Seoul National University, Seoul, South Korea

² Korea Institute of Fusion Energy, Daejeon, South Korea

³ Princeton University, Princeton, U.S.A.

Plasma current overshoot was proposed as an approach to enhance the confinement by increasing s/q with $q(0)$ near unity in ASDEX-Upgrade, JET, and KSTAR [1,2,3]. In the 2020 KSTAR campaign, plasma current overshoot (CuOv) discharges showed high performance of $\beta_N \lesssim 2.45$ and $H_{89} \lesssim 2.1$ during the main heating phase. Figure 1(a) compares a representative CuOv shot with the conventional one. From 2.4 s of discharge 25464, the ELM frequency increased and the line average density decreased while the neutron emission rate increased. Figure 1(b) shows q - and s/q profiles of discharge 25459 and 25464 obtained from MSE-EFIT. At 3.7 s, the q profile becomes broader, and an s/q value becomes larger than discharge 25459; however, these differences disappear at 4.6 s.

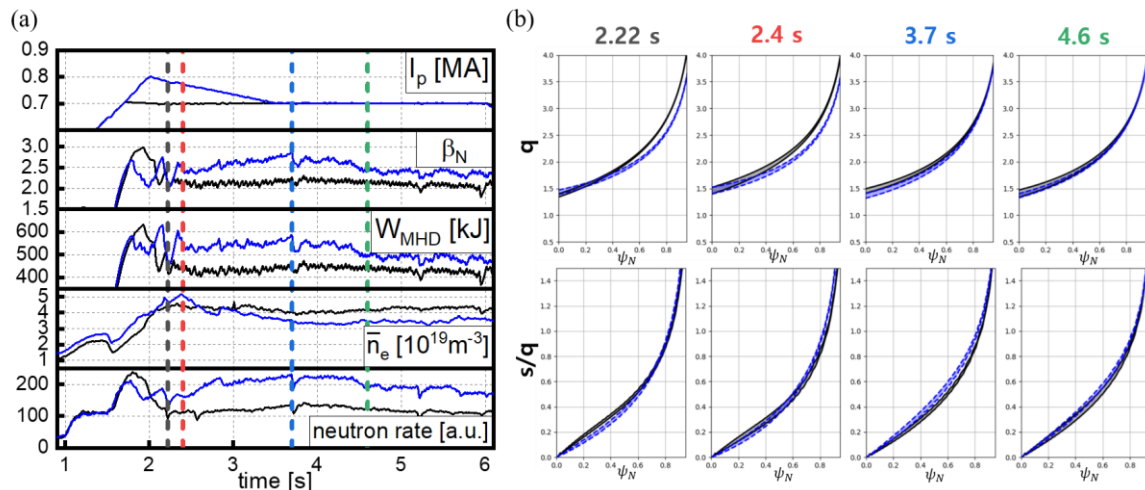


Fig. 1. (a) Comparison of 0D parameters between the representative CuOv case 25464 (Blue) and the conventional case 25459 without CuOv (Black). (b) q and s/q profile from MSE-EFIT of discharge 25464 (Blue) and 25459 (Black)

The characteristics of current overshoot discharge 25464 are as follows. From 2.4 s (red dashed vertical line in figure 2(a)) to 3.7 s (blue dashed vertical line in figure 2(a)), the total confinement enhancement factor, H_{89} increases with the thermal confinement enhancement factor, H_{98} . In other words, the thermal confinement enhancement contributes to the total energy confinement enhancement. However, it is difficult to distinguish if the fast ion confinement enhanced with the thermal energy confinement though the fast ion stored energy increases and contributes to the increase of the total energy while W_{thermal} decreases as shown

in figure 2(a). Meanwhile, as shown in figure 2(b) and (c), the core MHD mode switches from sawtooth to a fishbone-like mode from 2.7 s on discharge 25464.

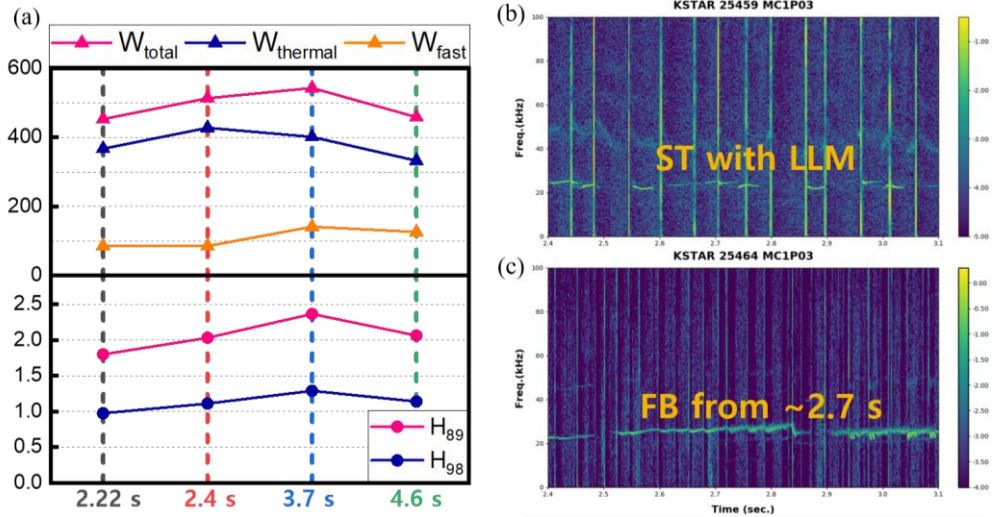


Fig. 2. (a) Thermal, fast ion, and total stored energy and energy confinement enhancement factors and (b) Mimov signal spectrogram in discharge 25459 (a) and discharge 25464 (b).

Further analysis of the effect of fast ion as well as s/q on the plasma performance is described below. Figure 3(a) and (b) show the q - and s/q profiles from kinetic-EFIT in order to reconstruct more delicate profiles. From 2.4 s to 3.7 s, the s/q value increases near $\rho_{\text{tor}} \sim 0.4 - 0.6$ and the edge region. Figure 3(c) shows the experimental R/L_{Ti} and the critical R/L_{Ti} , the ion temperature gradient (ITG) threshold expression $(R/L_{\text{Ti}})_c = (4/3) \times (T_{\text{i}}/T_{\text{e}} + 1) \times (1 + 2s/q)$ with $R/L_n < 2(1 + T_{\text{i}}/T_{\text{e}})$ [4].

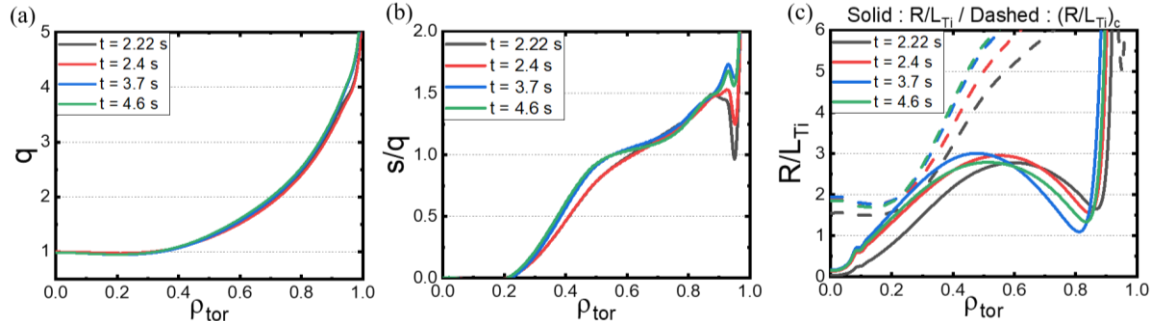


Fig. 3. (a) q - and (b) s/q -profile from kinetic-EFIT, (c) experimental ITG lengths, R/L_{Ti} and critical ITG lengths $(R/L_{\text{Ti}})_c$ from the theory [4] in discharge 25464.

The linear GKW simulation was performed at $\rho_{\text{tor}} = 0.4$ and 0.5, where R/L_{Ti} is close to $(R/L_{\text{Ti}})_c$. As shown in figure 4(a) and (b), the electromagnetic effect is dominated at 2.22 s and 2.4 s, then the fast ion effect prevails afterwards to stabilize the ITG mode. To investigate the effect of s/q , we scanned the magnetic shear only since the change of q values at $\rho_{\text{tor}} = 0.4$ and 0.5 were less than 1% at 2.4 s in discharge 25464. In the range in which the magnetic shear of 2.4 s and 3.7 s is located, the growth rate decreases as the shear increases. Based on these results, increasing s/q values can affect performance improvements between 2.4 s and 3.7 s.

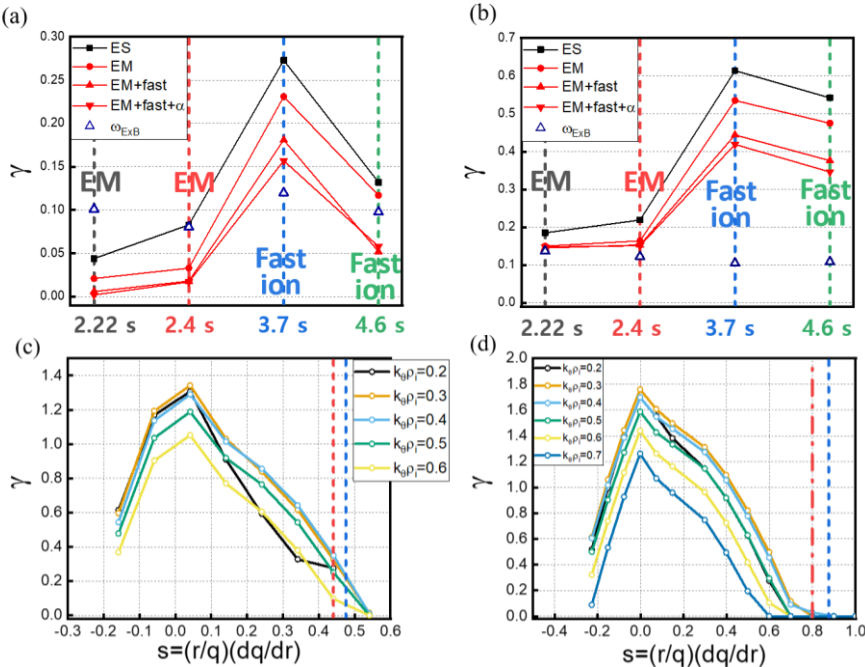


Fig. 4. Normalized linear growth rate at $\rho_{\text{tor}} = 0.4$ (a) and 0.5 (b) at 2.22, 2.4, 3.7 and 4.6 s of the most dominant mode from linear GKW simulations [5]. The most dominating stabilization effect of each time point is written in the figure. Normalized linear growth rate depending on magnetic shear at $\rho_{\text{tor}} = 0.4$ (c) and 0.5 (d) at 2.4 s in discharge 25464 where the red and the blue vertical line indicate the experimental magnetic shear at 2.4 s and 3.7 s, respectively. Here, we consider a circular $s - \alpha$ equilibrium model and the EM effect with various $k_{\theta}\rho_i$.

Now we investigate the pedestal effect. In figure 5(a), the PBM stability boundary narrows over time in discharge 25464. From 2.22 to 4.6 s, the mode number n of the most unstable PBM increases from 15 to 30, indicating the destabilization of high- n ballooning component with increased pedestal magnetic shear. This is a typical characteristic of the pedestal in the second stability regime [6]. As PBM exhibits more ballooning properties, the ELM frequency increases (figure 5(b)). It is noteworthy that the pedestal electron density decreases as ELM frequency increases, and the core electron density also decreases afterward (figure 6(a)). In figure 6(b), NUBEAM results show that the fast ion content can be increased by the reduced density. This may explain the increase of the neutron emission rate (figure 1(a)) [7] and the change in core MHD from sawtooth to the fishbone-like mode (figure 2(b) and (c)).

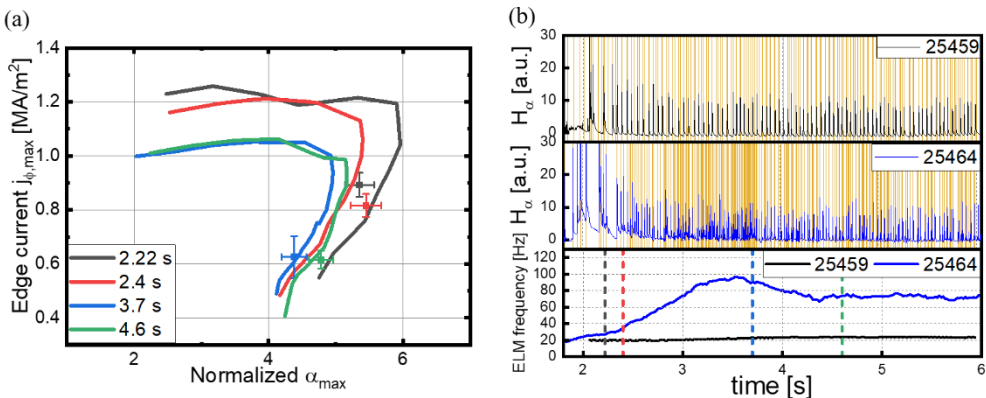


Fig. 5. (a) PBM stability at 2.22, 2.4, 3.7, 4.6 s in discharge 25464. (b) H_{α} signal and ELM frequency in discharge 25459 and 25464.

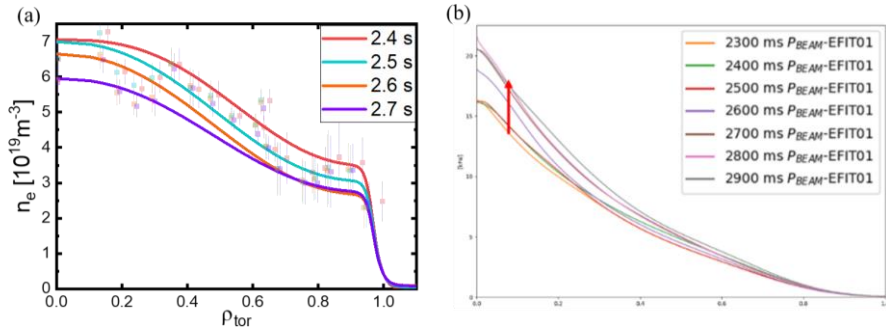


Fig. 7. (a) Time evolution of the n_e profile from TS and TCI system (b) and the fast ion pressure calculated by NUBEAM (c) from 2.4 s in discharge 25464.

We scanned the fast ion fraction at 4.6 s in discharge 25464 in the linear GKW simulation [5] to see the effect of the fast ion content to the microinstability stabilization. The fast ion fraction in discharge 25464 is larger than the conventional case 25517. The growth rate decreases as the fast ion fraction increases, as shown in figure 7; therefore, the increase in the fast ion fraction is thought to contribute to the performance improvement at 4.6 s of 25464.

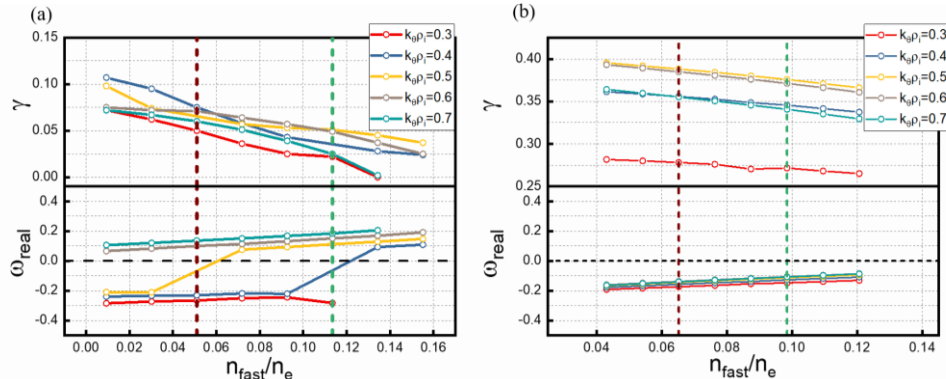


Fig. 7. Normalized linear growth rate and the frequency depending on the fast ion fraction at $\rho_{tor} = 0.4$ (a) and 0.5 (b) at 4.6 s in discharge 25464. Here, we consider the EM and fast ion effect with various $k_\theta \rho_i$. Here, the green correspond to 4.6 s in discharge 25464, and the wine-colored vertical line correspond to 4.6 s in the conventional case, discharge 25517.

Acknowledgment

This research was supported by National R&D program through the National Research Foundation of Korea (NRF) funded by the Ministry of Science & ICT (NRF-2019R1A2C1010757).

Reference

- [1] Citrin J. et al 2012 *Plasma Phys. Controlled Fusion* 54 065008
- [2] Hobirk J. et al 2012 *Plasma Phys. Controlled Fusion* 54 095001
- [3] Na Y.-S. et al 2020 *Nucl. Fusion* 60 086006
- [4] Guo S.C. and Romanelli F. 1993 *Phys. Plasmas* 5 520
- [5] Peeters A.G. et al 2009 *Comput. Phys. Commun.* 180 2650–72
- [6] Snyder P.B. et al 2002 *Phys. Plasmas* 9 2037
- [7] Lee Y.S. et al 2018 *Fusion Engineering and Design* 136 1112-1116